Journal Pre-proof

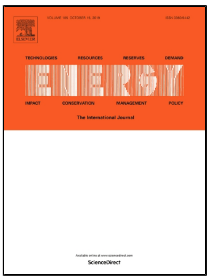

Opportunity Cost Including Short-Term Energy Storage in Hydrothermal Dispatch Models Using a Linked Representative Periods Approach

Diego A. Tejada-Arango, Sonja Wogrin, Afzal S. Siddiqui, Efraim Centeno

PII:	S0360-5442(19)31774-8
DOI:	https://doi.org/10.1016/j.energy.2019.116079
Article Number:	116079
Reference:	EGY 116079
To appear in:	*Energy*
Received Date:	24 October 2018
Accepted Date:	05 September 2019

Please cite this article as: Diego A. Tejada-Arango, Sonja Wogrin, Afzal S. Siddiqui, Efraim Centeno, Opportunity Cost Including Short-Term Energy Storage in Hydrothermal Dispatch Models Using a Linked Representative Periods Approach, *Energy* (2019), https://doi.org/10.1016/j.energy.2019.116079

Opportunity Cost Including Short-Term Energy Storage in Hydrothermal Dispatch Models Using a Linked Representative Periods Approach

Diego A. Tejada-Arango [a]*, Sonja Wogrin, Afzal S. Siddiqui [b], and Efraim Centeno

[a] *Instituto de Investigación Tecnológica, Universidad Pontificia Comillas, Spain*

[b] *Department of Statistical Science, University College London, United Kingdom, Department of Computer and Systems Sciences, Stockholm University,Sweden*

* Corresponding author. Diego.Tejada@iit.comillas.edu (D.A. Tejada-Arango)

Abstract

Short-term energy storage systems, e.g., batteries, are becoming one promising option to deal with flexibility requirements in power systems due to the accommodation of renewable energy sources. Previous works using medium- and long-term planning tools have modeled the interaction between short-term energy storage systems and seasonal storage (e.g., hydro reservoirs) but despite these developments, opportunity costs considering the impact of short-term energy storage systems in stochastic hydrothermal dispatch models have not been analyzed. This paper proposes a novel formulation to include short-term energy storage systems operational decisions in a stochastic hydrothermal dispatch model, which is based on a Linked Representative Periods approach. The Linked Representative Periods approach disposes of both intra- and inter-period storage constraints, which in turn allow to adequately represent both short- and long-term storage at the same time. Apart from the novelty of the model formulation itself, one of the main contributions of this research stems from the underlying economic information that can be extracted from the dual variables of the intra- and inter-period constraints, which allows to derive an hourly opportunity cost of storage. Such a detailed hourly economic value of storage has not been proposed before in the literature and is not possible in a classic Load Duration Curve model that does not adequately capture short-term operation. This advantage is reflected in the case study results. For instance, the model proposed in this paper and based on Linked Representative Periods obtains operating decisions of short-term energy storage systems with errors between 5% to 10%, while the classic Load Duration Curve approach fails by an error greater than 100%. Moreover, the Load Duration Curve model cannot determine opportunity costs on an hourly basis and underestimates these opportunity costs of hydro (also known as water value) by 6% to 24% for seasonal hydro reservoirs. The proposed Linked Representative Periods model produces an error on the opportunity cost of hydro units lower than 3%. Hourly opportunity costs for short-term battery energy storage systems using dual variables from both intra- and inter-period storage balance equations in the proposed model are also presented and

analyzed. The case study shows that the proposed approach successfully internalizes both short- and long-term opportunity costs of energy storage systems. These results are useful for planning and policy analysis, as well as for bidding strategies of ESS owners in day-ahead markets and not taking them into account may lead to infeasible operation or to suboptimal planning.

Keywords

energy storage systems, power system planning, hydrothermal dispatch, representative days, water value, opportunity cost.

1. Nomenclature

1.1 Indices

$p \in \mathcal{P}$	Periods (e.g., hours)
$m \in \mathcal{M}$	Months
$MP_{m,p}$	Set that relates hours and months
$w \in \mathcal{W}$	Type of day in the week (e.g., weekdays or weekend)
$l \in \mathcal{L}$	Load levels or load blocks
$rp \in \mathcal{RP}$	Representative periods (e.g., days)
$TM_{rp',rp}$	Set that relates transitions among rp
$k \in \mathcal{K}$	Hours inside a representative period
$CI_{p,rp,k}$	Set that relates hours with representative periods (i.e., cluster index)
$r \in \mathcal{R}$	Reservoirs
$g \in \mathcal{G}$	Generators
$t \subset g$	Subindex of Thermal units
$s \subset g$	Subindex of Storage units
$b \subset s$	Subindex of Short-term storage units (e.g., batteries)
$h \subset s$	Subindex of Hydro units
$HUR_{h,r}$	Set with hydro plants that are upstream of a reservoir
$HPR_{h,r}$	Set with pumped hydro plants that are upstream of a reservoir
$RUH_{r,h}$	Set with reservoirs that are upstream of a hydro plant
$RPH_{r,h}$	Set with reservoirs that are upstream of a pumped hydro plant
$RUR_{r,r}$	Set with reservoirs that are upstream of another reservoir

$\omega \in \Omega$	Scenarios
$a(\omega)$	Scenario tree relations

1.2 Parameters

d_*, o_*	Demand, operating reserve [MW]
wg_*	Load level duration or rp weight [h]
$\overline{p}_g$,$\underline{p}_g$	Maximum, minimum output [MW]
f_t, v_t	No load cost [$/h], variable cost [$/MWh]
su_t,sd_t	Startup, shutdown cost [$]
c_h,η_s	Production function and efficiency [p.u.]
$\overline{r}_r$,$\underline{r}_r$	Maximum and minimum storage level of the reservoir [hm3]
$r_r^{'}$	Initial and final storage level of the reservoir [hm3]
$\overline{soc}_b$,$\underline{soc}_b$	Maximum, minimum state of charge [p.u.]
$i^{\omega}_{*,r}$	Stochastic hydro inflows [m3/s]
p^{ω}_*	Scenario probability [p.u.]
$v^{'}$	Energy not served cost [$/MWh]
$v^{''}$	Operating reserve not served cost [$/MWh]

1.3 Variables

$UC^{\omega}_{*,t}$,$SU^{\omega}_{*,t}$,$SD^{\omega}_{*,t}$	Commitment, startup, and shutdown {0,1}
$P^{\omega}_{*,g}$	Production of generation units [MW]
$P^{'\omega}_{*,t}$	Production above minimum output [MW]
$C^{\omega}_{*,h}$, $C^{\omega}_{*,s}$	Consumption of a hydro/storage unit [MW]
$O^{\omega}_{*,g}$	Operating reserve of generation unit
$R^{intra,\omega}_{*,r}$,$R^{inter,\omega}_{*,r}$	Intra and inter reservoir level [hm3]
$S^{\omega}_{*,r}$	Reservoir spillage [hm3]
ENS^{ω}_*, RNS^{ω}_*	Energy and operating reserve not served [MW]
$SoC^{intra,\omega}_{*,b}$, $SoC^{inter,\omega}_{*,b}$	State-of-charge of a battery [p.u.]

In the previous nomenclature, "$*$" refers to the parameters used to identify time divisions: p for hours in the detailed model, (m,w,l) in the load-levels model, and (rp,k) in the linked representative periods model respectively.

2. Introduction

Due to climate policy and the increasing reduction of renewable investment costs, power systems are transitioning to accommodate wind and solar generation, which will require system flexibility for balancing requirements to

maintain system performance [1]. Most ways to determine the value of flexibility of a power system, are based in running Unit-Commitment (UC) models [2]. In this work, UC constraints are considered in order to represent the value of this flexibility as the short-term opportunity cost in hydrothermal dispatch models. Since the current technologies have limited technical capabilities to provide this flexibility, new alternatives are required. In this context, short-term storage systems, e.g., Battery-based Energy Storage Systems (BESS) or Pumped-hydro energy storage (PHS), are one of the most promising options that can deliver technical and economic benefits in the electric power sector such as providing the required flexibility and reducing system operational costs [3]. For instance, authors in [4] have shown that PHS reduces the operational cost by 2.5–11% in a wind power integration context for the Great Canary island in Spain. Therefore, there are significant short-term opportunity costs that should be considered in the medium- and long-term planning (e.g., hydrothermal dispatch is the focus in this paper). However, these opportunity costs are not properly considered or simplified in the classical hydrothermal models. In this context, both flexibility requirements and short-term storage systems operation require chronological information in order to be properly addressed in medium- and long-term planning models. Some authors have made an effort to make this analysis by using representative periods in their models. For instance, authors in [5] use a representative day to study the allocation and investment of ESS while authors in [6] focus on how to select the representative periods considering renewable energy sources. This is a common and valid assumption for power systems with a low share of hydro generation. However, hydrothermal power systems are highly dependent on seasonal hydro storage. Therefore, the interaction between short-term storage (intra-day or intra-week) and seasonal storage is relevant to co-optimize the use of hydro generators with short-term storage units that can provide similar services, such as energy arbitrage and operating reserves procurement for flexibility requirements [7].

This research focuses on the representation of short-term operational decisions in hydrothermal dispatch models, how these decisions change the operational decisions, and opportunity costs of seasonal storage. These results are useful for planning and policy analysis, as well as for bidding strategies of ESS owners in day-ahead markets and not taking them into account may lead to infeasible operation or to suboptimal planning. For instance, an underestimation of the opportunity cost in hydro generation during the operational planning may lead to use more hydro production, which could represent a risk for the power system during a dry season. The results in Section 6 show that classic hydrothermal dispatch models systematically underestimate the opportunity cost, while the proposed hydrothermal dispatch model significantly reduces this underestimation problem.

2.1 Literature Review

The hydrothermal dispatch problem aims at minimizing the total fuel cost of thermal generation units while properly dispatching the hydro and thermal generation units. There are two main types of models, the ones that are focused

on the long-term decision under hydro inflows uncertainty [8] and the ones that are focused on the short-term decisions considering detailed technical generation unit constraints [9].

On the one hand, the long-term hydrothermal dispatch problem aims at obtaining an optimal use of generation resources, most commonly under water inflows uncertainty, for the hydro and thermal generation units over a planning horizon considering multiple years [10]. Several models have been proposed for solving this problem in the literature, e.g., Ref. [8] is one of the classic references in this topic and more recently Ref. [11] gives a comprehensive review of different characteristics and model formulations on this topic. In addition, there are several commercial tools that aim to solve the hydrothermal dispatch problem that have been used in scientific research, such as: SDDP developed by PSR, PLEXOS Integrated Energy Model by Energy Exemplar, ProdRisk by SINTEF, NEWAVE by CEPEL [12], and StarNet Model by IIT [13]. For medium- or long-term studies, these tools use a Load Duration Curve (LDC) approach (also known as load-levels approach) with monthly or weekly stages. This is mainly due to the computational efficiency of LDC for large-scale systems. However, the LDC approach lacks chronological information within stages (e.g., weeks or months) and fails to represent short-term constraints (e.g., ramps, storage balance, etc.) [14].

On the other hand, the short-term hydrothermal dispatch aims at minimizing the fuel cost of thermal units for 1 day or 1 week while meeting various detailed hydraulic and electric system constraints, such as ramps, unit commitment [15], and nonlinear constraints of hydro units [9]. Although these approaches emphasize more the representation of short-term operation, they are not suitable to determine the opportunity cost of seasonal storage (also known as water value in the hydrothermal dispatch context) since their planning horizon covers only one week or less. However, short-term decisions may affect the operation of hydro reservoirs in the long term. Despite this situation, no relevant work has aimed to improve the representation of short-term operational decisions in long-term hydrothermal dispatch models. However and more recently, the *representative periods* (RP) method has been applied to long-term models in order to consider short-term decisions, such as renewable energy variability in the short-term [16] and UC constraints [17]. Generation dispatch and investment decisions are made for the selected periods (e.g., days or weeks) with a more detailed size of periods (hourly, for example). The RPs preserve the internal chronology of the hours, rendering a more realistic representation of changing storage levels over the course of a day or week. However, the basic definition of the RP does not preserve the chronology among them. Therefore, any Energy Storage System (ESS) with a full charge-discharge cycle longer than the RP (e.g., monthly or yearly) will not be adequately represented. In order to improve this situation, some authors have proposed methods to aggregate time series by modeling both intra-day and seasonal storage. For instance, the authors in [18] superpose inter-period and intra-period storage inventories to model short- and long-term ESS, while the authors in [19] proposed a hierarchical clustering method to maintain the chronology of the input time series

throughout the whole planning horizon to achieve the same goal. Moreover, the authors have proposed a linked RP model that also overcomes this shortcoming in [20]. Based on this last reference, a Linked Representative Periods (LRP) is proposed in this paper. By linking several RPs, it is possible to preserve some chronology among the RPs by superposing intra-period and inter-period storage balance equations. In addition, the selection of RPs is an important aspect of the RP approach. Some authors have proposed methods that optimize both the number and clustering of RPs to minimize the difference between the LDC and the approximate one created by the RPs [21]. The most versatile method for grouping RPs comes from [16] and relies on clustering techniques (e.g., k-means or k-medoids) to group a number of hours with any number of normalized characteristics (solar energy, demand, wind energy, etc.). Furthermore, several authors have debated about the optimal length for RPs [22]. For instance, in [23], the authors suggested representative groups of days or representative weeks, which gives the advantage of increasing the amount of chronology preserved. However, the effectiveness of linking shorter RPs versus longer RPs has not been analyzed in the LRP approach. The impact of the proposed model and the conclusions are analyzed in Section 8.

These recent developments in the representative periods can be applied to the hydrothermal dispatch problem framework in order to overcome the lack of detailed short-term decisions in long-term hydrothermal dispatch models. Despite these developments in short-term and seasonal storage interaction, in the literature opportunity costs in stochastic hydrothermal planning models have not been analyzed taking into account the possible interaction of short-term dynamics in the long term. This research article focuses on this gap. Moreover, the interpretation of opportunity costs for energy storage systems is not as intuitive as in the LDC models due to the superposition of both balance equations, i.e., intra-period and inter-period. Therefore, the opportunity cost for energy storage, considering short- (intra-period) and long-term (inter-period) operation is defined and analyzed in the proposed LRP model. This definition of the opportunity cost using both balance equations has not been determined before in the literature, which computes separately the short- and long-term opportunity costs for energy storage. These results can be used to improve the operational planning of hydrothermal power systems in the context of a high share of renewables energy sources and flexibility resources such as the BESS.

The challenge that have been tackled in this paper is to obtain the hourly opportunity cost for storage technologies that usually operate on very different time scales. For example, BESS might have a full charge/discharge cycle within a couple of hours or days, whereas a seasonal hydro storage facility – depending on the size of the reservoir – could have cycles of weeks, months or even years. Other important aspects of hydrothermal dispatch models such as uncertainty modeling [24] are out of its scope. A general formulation is proposed based on stochastic programming, which is compatible with different techniques to solve the dimensionality problem such as scenario reduction [25] and stochastic dual dynamic programming [26].

In this state-of-the-art context, the main contribution of this paper is the derivation and analysis of the hourly opportunity cost of storage technologies using the proposed LRP model, that improves the operational decisions in hydrothermal dispatch models. In other words, the LRP model can obtain an approximation of the ESS hourly opportunity cost within the studied time horizon without solving an hourly model. Moreover, the LRP model has the advantage that it obtains hourly detailed opportunity cost for different types of ESS technologies which operate on different time scales (hydro versus battery). This is a novel contribution since, so far, this has not been possible because classic LDC-type models lack chronological information among individual hours belonging to different load levels. Moreover, due to the reduction of temporal information in the proposed hydrothermal LRP model, this model is suitable for application on real-life case studies. This is relevant because it means that the proposed model can include short-term details that impacts the long-term operational and economic decisions without solving an hourly detailed model and in an efficient computational time.

An hourly model (HM) is used as a benchmark to compare our proposal to the classic LDC model and then to quantify the improvements in a stylized Spanish hydrothermal system. The HM can be solved for small case studies, however, in practice, for large-scale case studies it may not be possible to be solved.

The remainder of the paper is organized as follows: Sections 3 and 4 describe the main concepts in hydrothermal dispatch models and explain the main differences among the three models in this paper: the hourly model (HM) (the benchmark model), load duration curve model (LDC) (the classic model), and linked representative periods (LRP) (the novel model proposed in this paper). Section 5 defines the short-term storage value and water value definition for the LRP model. The definition of the hourly opportunity cost of different storage technologies represents one of the main contributions of this paper as it represents the storage opportunity cost extracted from hydrothermal dispatch models that accounts for both short- and long-term dynamics of the power system. Section 6 analyzes the results in a stylized Spanish case study based on European data for the year 2030. Section 7 discusses the coordination between short- and medium-term models in the LDC model and its equivalent in the proposed LRP model.

3. Hydrothermal Topology and Scenario Tree

In the context of hydrothermal dispatch, it is important to establish the hydro topology in order to determine the relationship among the water basins because of its impact on the dispatch and on the opportunity cost (also known as water value) in hydro generators. Fig. 1 shows an example hydro topology where three reservoirs (r1, r2, r3), including their hydro units (h1, h2, h3), are related among them. For instance, reservoir r3 receives its hydro inflows, turbined water and spilled water from reservoirs r1 and r2, and the pumped water from its own hydro unit h3.

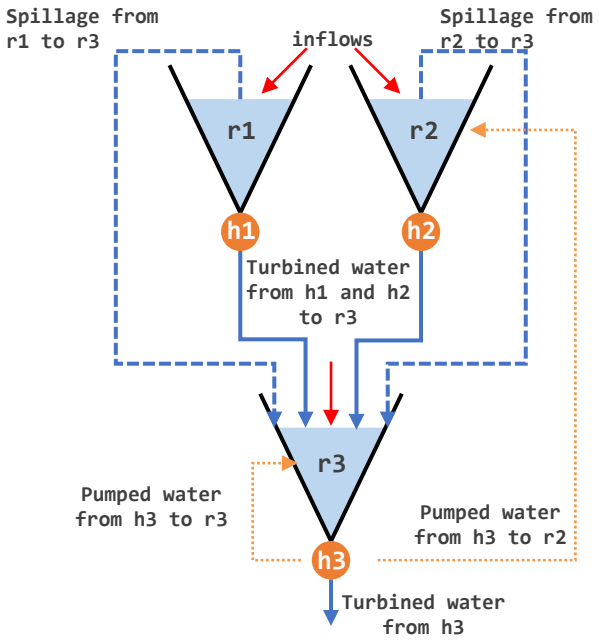

Fig. 1. Example of hydro topology or water basin

The main source of uncertainty in hydrothermal power systems is the water inflow [8]. This uncertainty is normally represented as a scenario tree [24], in which each node in the tree represents a hydro inflow level with a certain probability. In addition, the nodes are related among them, creating different scenarios to sample different realizations of the hydro inflows. Fig. 2 shows an example of a simple scenario tree with three scenarios: wet season, average inflows, dry season. In this example, the first stage decisions are taken in the first month represented in the tree (i.e., October) and the second stage decisions are taken for the following months. In addition, for each month in the second stage there are three different values of hydro inflows from each scenario.

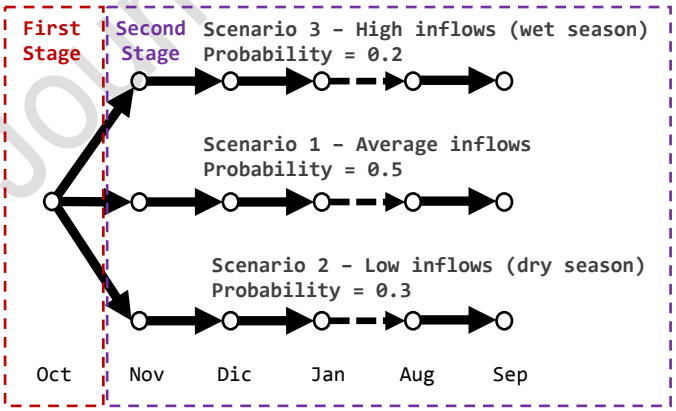

Fig. 2. Scenario tree example

Both hydro topology and scenario tree shown in this section are used as a reference in the remainder of this paper.

4. Model Formulation

Three optimization models are presented and solved in this paper using a stochastic formulation: An Hourly Model (HM), which is used as a benchmark, the classic Load Duration Curve (LDC) model, and the proposed Linked Representative Periods (LRP). The objective function and constraints of each model are detailed in the Appendix. Fig. 3 shows an overview of the analysis carried out in this paper. Hourly demand, wind, and solar time series are used as input data. Therefore, the HM model can be solved to obtain the benchmark results. In addition, two different clustering procedures are applied per each node of hydro inflow uncertainty, (i.e., per month) in order to obtain the input data necessary for the LDC and the LRP model respectively. First, individual hours are clustered in order to obtain the load levels for the LDC model per month. Second, the time series are grouped by periods (e.g., for the case study, representative days are considered) and then they are clustered in order to obtain the representative periods for the LRP model per month. Finally, the hourly results of each model are compared to determine the quality of the approximations in terms of objective function, productions, energy stored, and dual variables (e.g., prices, storage value, and water value).

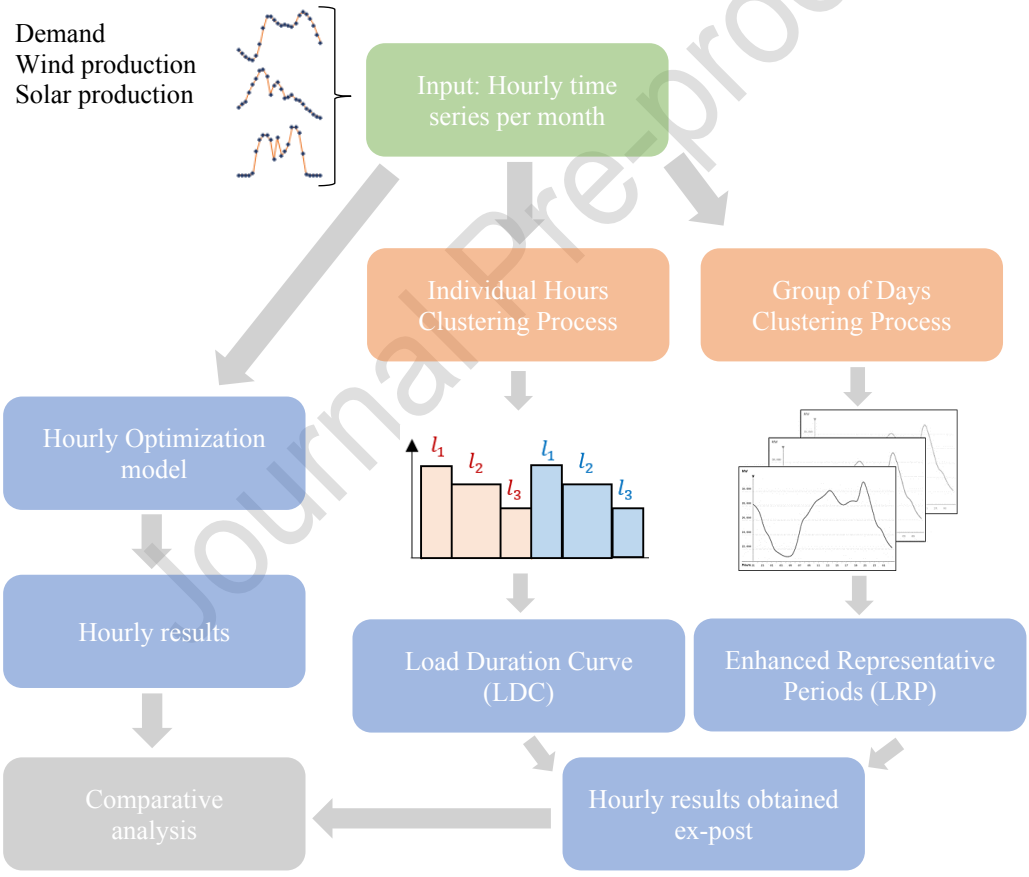

Fig. 3. Analysis overview: comparison of LDC and LRP models

It is important to highlight that both load levels and representative periods are selected per month because the uncertainty in the hydro inflows is per month, see Fig. 2. Scenario tree example

Therefore, the load levels and representative periods are different among months. This is guaranteed through a time division structure in both models. Fig. 4 shows an example of the structure of the LDC model, where two

months (m_1, m_2) have a subdivision in weekdays (w_1) and weekend (w_2), each one with three different load levels (l_1, l_2, l_3).

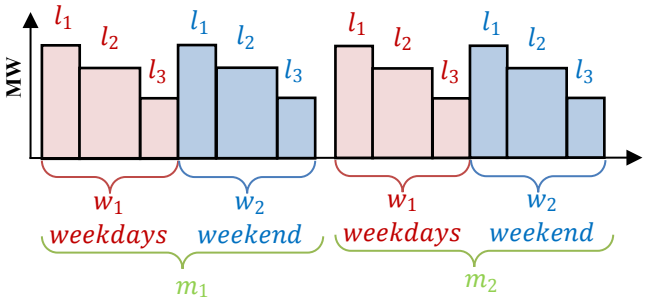

Fig. 4. Structure of LDC time division

Fig. 5 shows an example of the structure for the LRP model, where the two months have their own representative periods (i.e., rp_1 and rp_2 for m_1, and rp_3 and rp_4 for m_2), each one with a set of chronological hours (k_1 to k_{24} in a 24-hour representative period example).

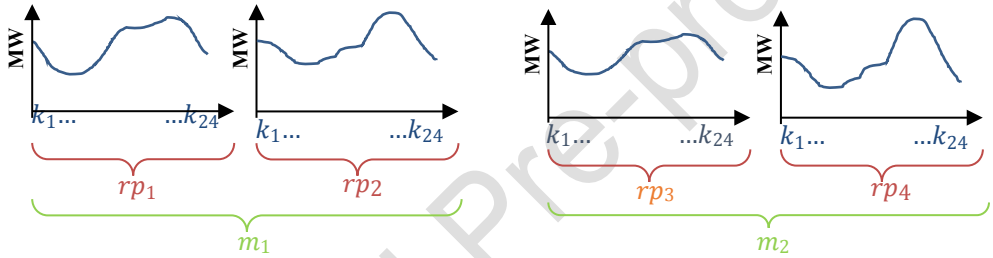

Fig. 5. Structure of LRP time division

These time divisions facilitate the formulation of storage balance constraints in both models considering the scenario-tree structure. Sections 4.1 to 4.8 show the storage balance constraints in the three optimization models. Although the detailed optimization models are shown in appendices A to C, the storage balance equations are shown here to help understand the analysis in the following sections.

4.1 Long-term Energy Storage Balance Constraint in the Hourly Model

$$R_{p-1r}^{intra,\omega'} - R_{pr}^{intra,\omega} + i_{pr}^{\omega} - S_{pr}^{\omega} + \underbrace{\sum_{r' \in RUR_{r',r}} S_{pr'}^{\omega}}_{Water\ spillage\ from\ upstream\ reservoirs} + \underbrace{\sum_{h \in HUR_{h,r}} P_{ph}^{\omega}/c_h}_{Turbined\ water\ from\ upstream\ hydro\ plants} - \underbrace{\sum_{h \in RUH_{r,h}} P_{ph}^{\omega}/c_h}_{Turbined\ water\ from\ hydro\ plants\ in\ reservoir\ r} + \underbrace{\sum_{h \in HPR_{h,r}} C_{ph}^{\omega}/c_h}_{Pumped\ water\ from\ hydro\ plants\ to\ reservoir\ r} - \underbrace{\sum_{h \in RPH_{r,h}} C_{ph}^{\omega}/c_h}_{Pumped\ water\ to\ other\ reservoirs} = 0 \quad \forall \omega pr \ \ \omega' \epsilon\, a(\omega) \tag{1}$$

4.2 Short-term Energy Storage Balance Constraint in the Hourly Model

$$SoC_{p-1b}^{intra,\omega'} - SoC_{pb}^{intra,\omega} - P_{pb}^{\omega} + C_{pb}^{\omega} = 0 \quad \forall \omega pb \quad \omega' \epsilon\, a(\omega) \tag{2}$$

4.3 Long-term Energy Storage Balance Constraint in the Load Duration Curve

$$R^{inter,\omega'}_{m-1r} - R^{inter,\omega}_{mr} + i^{\omega}_{mr} - S^{\omega}_{mr} + \underbrace{\sum_{r' \in RUR_{r',r}} S^{\omega}_{mr'}}_{Water\ spillage\ from\ upstream\ reservoirs} + \underbrace{\sum_{wl}\sum_{h \in HUR_{h,r}} wg_{mwl} \cdot P^{\omega}_{mwlh} / c_h}_{Turbined\ water\ from\ upstream\ hydro\ plants} - \underbrace{\sum_{wl}\sum_{h \in RUH_{r,h}} wg_{mwl} \cdot P^{\omega}_{mwlh} / c_h}_{Turbined\ water\ from\ hydro\ plants\ in\ reservoir\ r} + \underbrace{\sum_{wl}\sum_{h \in HPR_{h,r}} wg_{mwl} \cdot C^{\omega}_{mwlh} / c_h}_{Pumped\ water\ from\ hydro\ plants\ to\ reservoir\ r} - \underbrace{\sum_{wl}\sum_{h \in RPH_{r,h}} wg_{mwl} \cdot C^{\omega}_{mwlh} / c_h}_{Pumped\ water\ to\ other\ reservoirs} = 0 \quad \forall \omega mr \quad \omega' \epsilon\, a(\omega) \tag{3}$$

4.4 Short-term Energy Storage Balance Constraint in the Load Duration Curve

$$SoC^{inter,\omega'}_{m-1b} - SoC^{inter,\omega}_{mb} - \sum_{wl} wg_{mwl} \cdot P^{\omega}_{mwlb} + \sum_{wl} wg_{mwl} \cdot C^{\omega}_{mwlb} = 0 \quad \forall \omega mb \quad \omega' \epsilon\, a(\omega) \tag{4}$$

4.5 Intra-period Balance Constraint for Long-term Energy Storage in the Linked Representative Periods

$$R^{intra,\omega'}_{rp,k-1,r} - R^{intra,\omega}_{rp,k,r} + i^{\omega}_{rp,k,r} - S^{\omega}_{rp,k,r} + \underbrace{\sum_{r' \in RUR_{r',r}} S^{\omega}_{rp,k,r'}}_{Water\ spillage\ from\ upstream\ reservoirs} + \underbrace{\sum_{h \in HUR_{h,r}} P^{\omega}_{rp,k,h} / c_h}_{Turbined\ water\ from\ upstream\ hydro\ plants} - \underbrace{\sum_{h \in RUH_{r,h}} P^{\omega}_{rp,k,h} / c_h}_{Turbined\ water\ from\ hydro\ plants\ in\ reservoir\ r} + \underbrace{\sum_{h \in HPR_{h,r}} C^{\omega}_{rp,k,h} / c_h}_{Pumped\ water\ from\ hydro\ plants\ to\ reservoir\ r} - \underbrace{\sum_{h \in RPH_{r,h}} C^{\omega}_{rp,k,h} / c_h}_{Pumped\ water\ to\ other\ reservoirs} = 0 \quad \forall \omega, rp, k, r \quad \omega' \epsilon\, a(\omega) \tag{5}$$

4.6 Inter-period Balance Constraint for Long-term Energy Storage in the Linked Representative Periods

$$R^{inter,\omega'}_{m-1,r} - R^{inter,\omega}_{mr} + \sum_{(rp,k) \in \{CI_{p,rp,k} \cap MP_{m,p}\}} \left[R^{intra,\omega}_{rp,k,r} - R^{intra,\omega'}_{rp,k-1,r}\right] = 0 \quad \forall \omega mr \quad \omega' \epsilon\, a(\omega) \tag{6}$$

4.7 Intra-period Balance Constraint for Short-term Energy Storage in the Linked Representative Periods

$$SoC^{intra,\omega'}_{rp,k-1,b} - SoC^{intra,\omega}_{rp,k,b} - P^{\omega}_{rp,k,b} + C^{\omega}_{rp,k,b} = 0 \quad \forall \omega, rp, k, b \quad \omega' \epsilon\, a(\omega) \tag{7}$$

4.8 Inter-period Balance Constraint for Short-term Energy Storage in the Linked Representative Periods

$$SoC^{inter,\omega'}_{m-1,b} - SoC^{inter,\omega}_{mb} + \sum_{(rp,k) \in \{CI_{p,rp,k} \cap MP_{m,p}\}} \left[SoC^{intra,\omega}_{rp,k,r} - SoC^{intra,\omega'}_{rp,k-1,r}\right] = 0 \quad \forall \omega mb \quad \omega' \epsilon\, a(\omega) \tag{8}$$

4.9 Comparison of Storage Balance Constraints Among the Models

Here the previous constraints are analyzed for each model. First, in the *HM* model, the storage balance constraints are imposed for each period p, equations (1) and (2). Therefore, reservoir level and SoC are determined for each hour in the time horizon. These results are used as a benchmark to test the LDC and LRP model, see Fig. 3. Constraints for LTESS and STESS are stated for $\omega' \epsilon\, a(\omega)$, which allows to relate the different scenarios through the scenario tree. For instance, Fig. 2 shows a scenario tree with three scenarios: wet season, average inflows, dry season. In this example, the ancestor $a(\omega)$ of scenario 3 in November is scenario 1 in October. Therefore, the set $a(\omega)$ is relating a scenario with the corresponding predecessor scenario in the tree.

Second, in the *LDC* model, both storage balance equations (3) and (4) (i.e., LTESS and STESS) include the load-level duration (wg_{mwl}) to consider the number of hours that are represented for each load level. In other words, the multiplication by wg_{mwl} guarantees that all the charged/discharged energy is considered within the month m. These

equations are for the inter-period variables. Intra-period variables are not available in this model due to the lack of chronology within the month m.

Third, in the *LRP* model, the storage balance constraints are defined for inter- and intra-periods, equations (5)-(8). These equations create the continuity in storage across the entire time horizon that allows for the modeling of short-term and long-term storage simultaneously. Intra-period constraints (7)-(8) ensure the storage balance within the RP, while inter-period constraints guarantee the storage balance between representative periods by checking at regular intervals (e.g., aggregation of hours such as months m) that all the energy charged and discharged since the previous month plus the total energy at the last checkpoint are within bounds. This is possible because the cluster index, $CI_{p,rp,k}$, and the relationship between periods and months, $MP_{m,p}$, are known as a result of the clustering procedure to determine the RPs. The intersection of both sets $\{CI_{p,rp,k} \cap MP_{m,p}\}$ indicates which RPs belong to the month and, therefore, must be considered in the inter-period balance.

Finally, notice that constraints for LTESS and STESS are equivalent if, for example, a hydro reservoir has a pump unit which is not in a hydro basin and it has no hydro inflows. However, both constraints are kept in order to facilitate the distinction between both types of storage technologies. In real hydro power plants, there is a nonlinear dependence between the reservoir head and the reservoir volume [13]. Nevertheless, and for the sake of simplicity in storage balance constraints for LTESS, a linear function of the turbine outflow is assumed. Although nonlinear dependence could be considered at the expense of more complex optimization models such as in [13].

5. Analysis of Energy Storage Opportunity Cost

The energy storage opportunity cost is the substitution cost of the stored energy that can be calculated as the decrease on total system cost when an extra energy storage unit is available, also known as dual approach [27]. In hydrothermal dispatch context, this value is determined by the thermal generation unit that is replaced by the energy storage unit, i.e., hydro generation.

In Section 4, three models have been formulated for the hydrothermal dispatch as Mixed Integer Programming (MIP) problems. This is a frequent approach in short-term hydrothermal scheduling in order to consider practical limitations of the generation units such as ramps and UC constraints [28]. However, as it is mentioned in [27], the value of dual variables in a MIP is not well-defined. Hence, it is a common practice to approximate the dual variables of interest by fixing the integer variables (e.g., commitment decisions) obtained in the MIP solution and then solving the model again as a Linear Programming (LP) problem [13]. Under this assumption, the opportunity cost of ESS can be obtained from the dual variable of the storage balance equations of each model, while the opportunity cost of hydro reservoirs is normally called water value [27]. However, the name *water value* cannot be applied to BESS since there are no hydro inflows for this type of technology. Instead, the *storage value* is used to describe the opportunity cost of short-term storage (i.e., BESS).

- *Hourly Model (HM)*: The opportunity cost for each type of storage is obtained from the dual variables of equations (1) and (2). Therefore, water value $\left(\mu_{pr}^{intra,\omega}\right)$ is obtained from (1) and storage value $\left(\mu_{pb}^{intra,\omega}\right)$ from (2). These opportunity costs are for each hour in the time horizon.
- *Load Duration Curve Model (LDC)*: Water value $\left(\mu_{mr}^{inter,\omega}\right)$ is obtained from (3) and storage value $\left(\mu_{mb}^{inter,\omega}\right)$ from (4). Since there is no chronology between load levels, the opportunity cost for each type of storage is obtained only for an aggregation of hours (e.g., months).
- *Linked Representative Periods Model (LRP)*: This model has two balance equations for each storage technology. One for the storage balance inside the representative period (intra-period) and another for the storage balance through the aggregation of hours in the time horizon (inter-period). Each balance equation has its dual variable; however, the combination of both dual variables is necessary to determine the hourly dual variable that is comparable to the one obtained from the HM model. Equation (9) defines the hourly storage/water value for short- and long-term storage using the LRP model. $\mu_{rp,k,s}^{intra,\omega}$ is obtained from the dual variables of (5) and (7) for hydro reservoirs and BESS, respectively. In the same way, $\mu_{m,s}^{inter,\omega}$ is obtained from the dual variables of (6) and (8). Equation (9) shows the opportunity cost of energy storage as a linear combination of short- (intra-period balance) and long-term decisions (inter-period balance). Therefore, the LRP model distinguishes the impact of short-term decisions within the total opportunity cost, which is not possible in the HM model. Section 7 shows the relevance of (9) in the opportunity cost of storage since it allows to differentiate the share of short- and long-term economic information in this opportunity cost.

$$\mu_{ps}^{intra,\omega} = \sum_{(rp,k)\in CI_{p,rp,k}} \sum_{m\in MP_{m,p}} \frac{1}{p_m^{\omega}} \cdot \left(\frac{\mu_{rp,k,s}^{intra,\omega}}{wg_{rp}} + \mu_{m,s}^{inter,\omega} \right) \quad \forall \omega ps \tag{9}$$

6. Case study and Results

As a case study, a stylized Spanish power system in target year 2030 is chosen. The Spanish case is relevant because it has hydro reservoirs (i.e., seasonal storage) and, according to ENTSO-E [29], the next ten years will likely bring investment in Battery Energy Storage System (BESS), i.e., short-term energy storage. The wind and solar profiles were taken from [30] and [31] respectively, while hourly demand data and annual production per technology were taken from the vision 1 in the ENTSO-E *Ten Year Network Development Plan 2016* [29]. For the sake of simplicity, the case study is represented as a single node example. The transmission network may change the results in the case study, especially if there is any congestion; however, since transmission network constraints have already been successfully included in the classic hydrothermal LDC model [32] as well as in the former version of the LRP model [20], they are omitted here. In addition, Ref. [33] shows that network congestion improves the

accuracy of the clustering techniques to reduce temporal information, such as the ones used in this paper for the proposed hydrothermal LRP model.

The water basin is represented by three reservoirs. Reservoirs 1 and 2 are upstream of reservoir 3, and, therefore, reservoir 3 receives, besides its hydro inflows, the hydro production and water spillage from reservoirs 1 and 2, such as in Fig. 1. The scenario tree is a simplified structure of three scenarios in order to consider monthly hydro inflows in dry, average, and wet seasons, see Fig. 2. The probabilities for each scenario are 30%, 50%, and 20%, respectively. The first-stage decision is taken for October[1] and second-stage decisions are taken from November to September. For the sake of simplicity, the stability of the solution for different scenario trees is not verified. This will be addressed in future research to determine the impact of different scenario trees in the results.

Load levels and representative periods are obtained via the k-means clustering procedure for each month. The clusters were chosen by normalizing time series for the hourly demand, wind availability, and solar availability, see Fig. 3. For the LL model, 12 load levels (6 for weekdays and 6 for the weekend) per month have been defined. For the LRP model, some sensitivities for the selection of the representative periods have been defined: 1 representative period with 24h per month (1RPx24h), 1 rp with 48h per month (1RPx48h), 1 rp with 96h per month (1RPx96h), 2 rp with 24h per month (2RPx24h), and 4 rp with 24h per month (4RPx24h). These sensitivities are performed in order to identify if it is better to have only one rp per month sharing information or to have more rp per month sharing information among them and between months. Based on previous results in [20], more rp per month sharing information may be better than one rp per month.

Finally, a BESS with a power rating of 200MW, energy capacity of 4 hours, and round-trip efficiency of 90% is considered. The BESS is installed to deal with hourly variation of variable renewable energy sources.

6.1 Objective Function and Time to Solve

Table 1 shows the results using as a reference the results obtained for the HM. The objective function error is calculated using the value of the objective function of the hourly model as the theoretical value, while the CPU time is shown as a fraction of the time taken by the hourly model to solve the problem. All models were solved until optimality, i.e., until either their optimal point or the integrality gap equaled zero.

The analysis of the results shows two main situations. First, the LRP 4RPx24h as the best performance in terms of the objective function. The objective function error is lower than 1% compared to the HM model, and it only takes one tenth of the time to solve. In addition, all the LRP results for the different sensitivities have objective function errors lower than 4%. Second, although the LDC is one of the fastest models to solve the problem, its objective

[1] October is the beginning of the hydrological year in Spain.

function error exceeds 10%.[2] Therefore, the LRP improves the results of the hydrothermal dispatch problem without hampering the computational efficiency.

The results obtained for the sensitivities of the LRP model confirm that more rps per month sharing information is better than one longer rp per month. For instance, the 1RPx48h and 2RPx24h take the same number of hours per month and produce similar CPU time performance. However, the objective function error in 2RPx24h is half of that obtained with 1RPx48h. Therefore, and for the sake of simplicity, only the LRP 4RPx24h model results are shown in the following sections.

Table 1. Objective Function Error and CPU Time

	LRP 4RPx24h	LRP 2RPx24h	LRP 1RPx96h	LRP 1RPx48h	LRP 1RPx24h	LDC
OF Error [%]	0.1	1.7	3.4	3.6	3.6	11.7
CPU Time [p.u.]	0.10	0.02	0.05	0.02	0.01	0.01

6.2 First- and Second-Stage Production Results

Table 2 shows the errors in production per technology for both LDC and LRP model. Negative values indicate an underestimation in comparison to the HM result, while positive values indicate an overestimation. The black color is used to highlight absolute values lower or equal to 5%, light orange color for absolute values greater than 5% and lower or equal to 10%, and the dark red color for absolute values higher than 10%. Technologies such as coal and fuel oil are not shown because their total production is negligible. Additionally, technologies such as wind, solar, and run-of-river are also not shown, in this case because the total production error is lower than 1% in both models.

The results are classified into two groups: first and second stage. The LRP model has better results than LDC model in both groups. In fact, BESS production error in the LRP model is almost ten times lower than the result with the LDC model for the first stage, and almost twenty times smaller for the second stage. The Open Cycle Gas Turbine (OCGT) is more difficult to estimate in both models because it is the peak technology, and yet the LRP improves the approximation made by the LDC.

The LDC model underestimates Combined Cycle Gas Turbine (CCGT) production (marginal technology most of the time) due to the loss of chronology among the load levels that overestimates BESS production, see Table 2. This leads to an underestimation of BESS storage values, see Table 2. On the other hand, the CCGT production error in the LRP model is lower than 5% as well as the BESS storage value in Table thanks to the more accurate

[2] Considering twice the number of LL, the LDC objective function error reduces to an error of 6%, but the CPU time increases six-fold.

representation of chronological constraints. These results show the interdependence between the marginal technologies and the BESS storage value.

Table 2. Total Production Error per Technology [%]

Tech	First Stage		Second Stage	
	LDC	LRP	LDC	LRP
Nuclear	4.6	1.7	Sc1 2.9	Sc1 -0.3
			Sc2 2.8	Sc2 -0.4
			Sc3 3.3	Sc3 -0.7
CCGT	-35.8	-0.5	Sc1 -8.6	Sc1 -3.5
			Sc2 -5.7	Sc2 -4.4
			Sc3 -6.8	Sc3 -2.6
OCGT	-30.7	-22.7	Sc1 -68.4	Sc1 -49.0
			Sc2 -44.3	Sc2 -0.5
			Sc3 -68.8	Sc3 -16.9
Hydro	-5.5	-4.3	Sc1 -0.4	Sc1 -0.3
			Sc2 0.6	Sc2 -0.5
			Sc3 -0.3	Sc3 -0.3
BESS	110.9	9.1	Sc1 133.9	Sc1 -5.4
			Sc2 115.1	Sc2 -5.1
			Sc3 123.7	Sc3 4.6

6.3 Hydro Reservoir and State-of-Charge Results

In this section, the storage level is analyzed for both technologies, i.e., hydro (seasonal storage) and BESS (short-term storage). First, storage level for hydro reservoir is approximated with more accuracy in the LRP model compared to the LDC model. For instance, Fig. 6 (top) shows the storage level for reservoir 2 in scenario 1 for both models in comparison to the HM model. The storage-level-average error over all the scenarios and reservoirs is 4.5% for the LRP model and 9.0% for the LDC model. Therefore, the LRP model is twice as accurate as the LDC model for the reservoir levels.

Second, the hourly BESS SoC can be obtained for the LRP model, which is not possible with the LDC model. Fig. 6 (middle) shows the hourly evolution of the SoC in a particular week for the HM and the LRP model. It is possible to observe the daily cycles of the BESS and how the LRP model results mimic the HM solution. The total number

of cycles[3] obtained from each model in the target year are compared in Fig. 6 (bottom). This figure shows the total number of cycles per scenario for each model. The total number of cycles determined from the LDC results doubles the number obtained with the HM model, which was expected due to the overestimation in the BESS production shown in Table 2. By contrast, the average error in the number of cycles for the LRP model is 5%. This result is important because the number of cycles is key to determine replacement or maintenance in BESS.

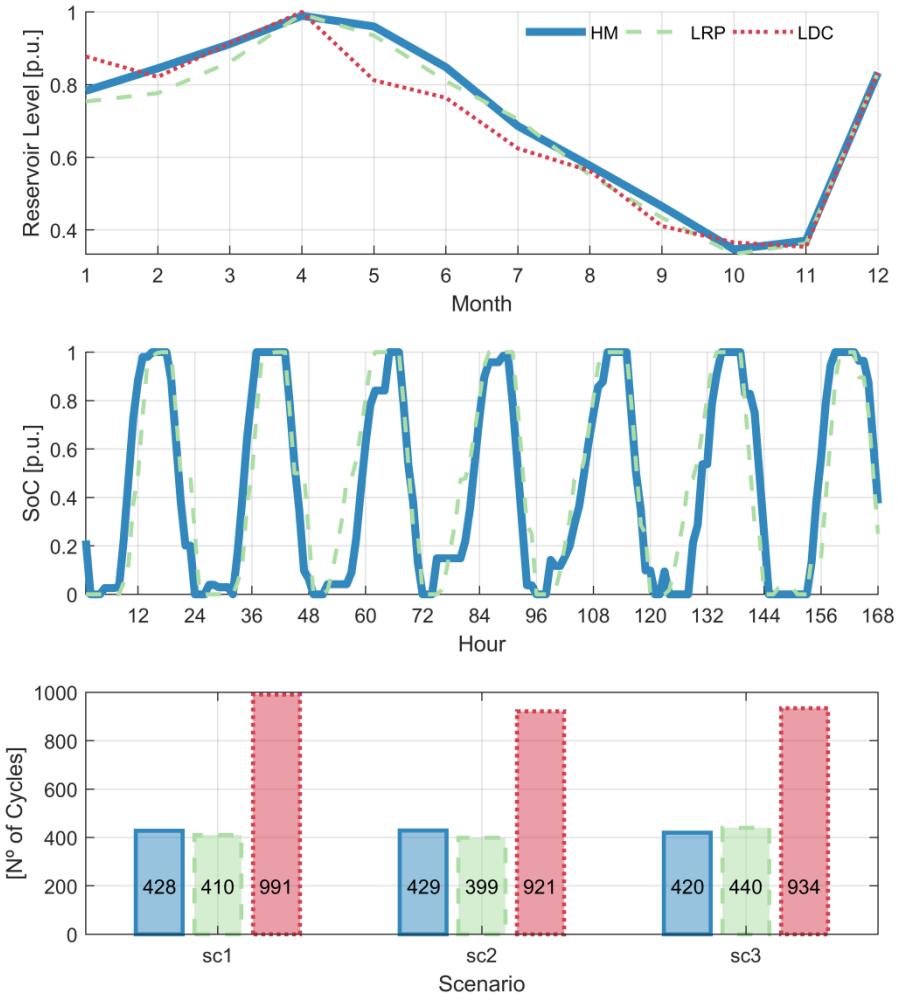

Fig. 6. Reservoir Level [p.u.] (top). BESS SoC [p.u.] over a week (middle). Total number of cycles for the BESS (bottom)

6.4 Marginal and Opportunity Costs

Table 3 shows the errors with Stochastic Marginal Cost (SMC) and Opportunity Cost (OP). The HM results have been chosen as a reference for the error calculation. The SMC is calculated as the weighted dual variable from the balance equation in each model. The OP is calculated as the weighted dual variable from the inter-period storage

[3] The cycles are estimated for all models using the total charge/discharge energy over the year and dividing it by the BESS' maximum energy capacity.

balance equation in each model, equations (3), (4), (6), and (8). The same color notation as in Table 2 is used. On the one hand, the LRP model mostly leads to errors lower than 5% and is the most accurate model in almost all results. On the other hand, the LDC model yields in most of the cases errors higher than 10% and, as expected from the results in previous sections, exhibits the worst performance in the opportunity cost of the BESS throughout the time horizon, overestimating most of the months the economic signal of energy storage.

Table 3. Stochastic Marginal Cost and Opportunity Cost Results – Error [%]

Month	SMC		OP Res 1		OP Res 2		OP Res 3		OP BESS	
	LDC	LRP	LDC	LRP	LDC	LRP	LDC	LRP	LDC	LRP
Oct	-13.7	1.3	-16.3	-0.6	-6.6	-0.6	-23.9	2.8	-6.7	-2.0
Nov	-4.7	-2.0	-16.3	-0.6	-6.6	-0.6	-23.9	2.8	-4.7	-0.4
Dec	-28.5	0.3	-16.3	-0.6	-6.6	-0.6	-23.9	2.8	-16.3	-3.6
Jan	-10.8	-1.3	-17.7	-2.4	-8.2	-2.4	-22.6	-1.2	-32.2	-0.9
Feb	-8.7	0.7	-12.5	-0.4	-8.2	-0.4	-22.6	-1.0	-32.4	-3.1
Mar	-13.5	6.6	-12.5	-0.4	-8.2	-0.4	-21.4	-1.0	-27.4	5.6
Apr	-9.5	0.6	-12.5	-0.4	-8.2	-0.4	-21.4	-1.0	-29.0	-3.2
May	-14.0	0.2	-12.5	-0.4	-8.2	-0.4	-21.4	-1.0	-26.7	0.0
Jun	-9.4	1.4	-12.5	-0.4	-8.2	-0.4	-21.4	-1.0	-26.3	4.3
Jul	-23.1	2.0	-12.5	-0.4	-8.2	-0.4	-21.4	-1.0	-37.9	4.3
Aug	-13.8	4.7	-11.9	1.2	-6.9	-0.6	-22.3	-1.4	-30.2	1.9
Sep	-15.0	1.5	15.4	0.4	-6.9	-0.6	6.0	0.3	-28.8	-0.9
Mean Absolute Error	13.7	1.9	14.1	0.7	7.6	0.7	21.0	1.4	24.9	2.5

The errors in reservoir 3 are higher than those in reservoir 1 and 2. This is a reasonable result, considering that reservoir 3 is downstream of reservoir 1 and 2. Therefore, errors in reservoirs 1 and 2 propagate to reservoir 3 and complicate the estimation.

In Section 5, the equation (9) has been presented, which allows us to determine the intra-period or hourly opportunity cost in the LRP model. This represents the main advantage over the LDC. Fig. 7 shows the opportunity cost (or storage value) of BESS in the HM, LRP, and LDC models for a particular week. The opportunity cost obtained from the LRP model mimics the trend followed by the results in the HM model. In fact, almost 75% of the time, the difference between the results of both models is lower than 10%. Fig. 7 shows one value for the LDC model throughout the week because it only determines one opportunity cost value per month, see equations (3) and (4).

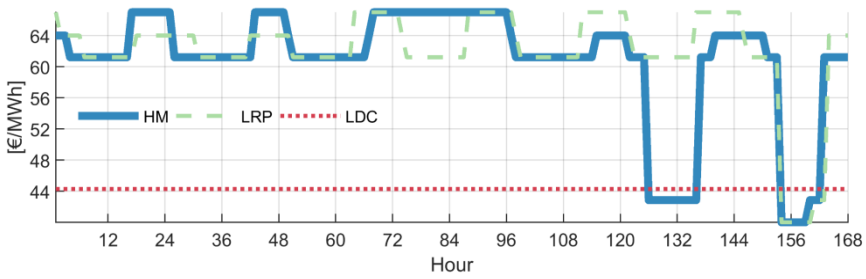

Fig. 7. Opportunity Cost or Storage Value of BESS [€/MWh]

7. Discussion

The main drawback of the previous result is that the medium-term model, i.e., LDC model, does not consider short-term chronological information. In fact, as shown in Section 6, the LDC model has the worst performance. All the time resolutions tested for the LRP model have shown a better performance than the LDC model. This means that LRP succeeds in the internalization of short-term chronological information in the medium-term hydrothermal problem, which enables inclusion of the operation of BESS without solving the HM model for the entire medium-term horizon. In other words, the LRP model co-optimizes both medium- (or long-) and short-term decisions. Moreover, equation (9) in the LRP has the advantage that it allows to differentiate between both components: intra-period and inter-period opportunity cost and therefore, know the share of each component in the total opportunity cost. Fig. 8 (top) shows the share of these components in the E-RP model for the same week in Fig. 7. Most of the time, the inter-period value represents more than 90% of the total value through the week, while the intra-period value gets more relevance, near 40%, at the end of the week (around hour 156), when the opportunity cost has the biggest change in Fig. 7. However, this share in the composition cannot be taken as a general behavior. For instance, Fig. 8 (bottom) shows results for another week in the same case study. Here, it can be observed that there are hours where the intra-period represents the 100% of the total value of the opportunity cost in the BESS. Therefore, the share changes depending on the characteristics of the case study as well as the location within the time scope. These types of results and analysis cannot be developed in the classic LDC model and represent a novel contribution in this research. This contribution opens the door to new analysis and studies. For instance, these results give insights to market participants of when short-term storage opportunities are more relevant than long-term storage opportunities and then considering this situation in their market bids.

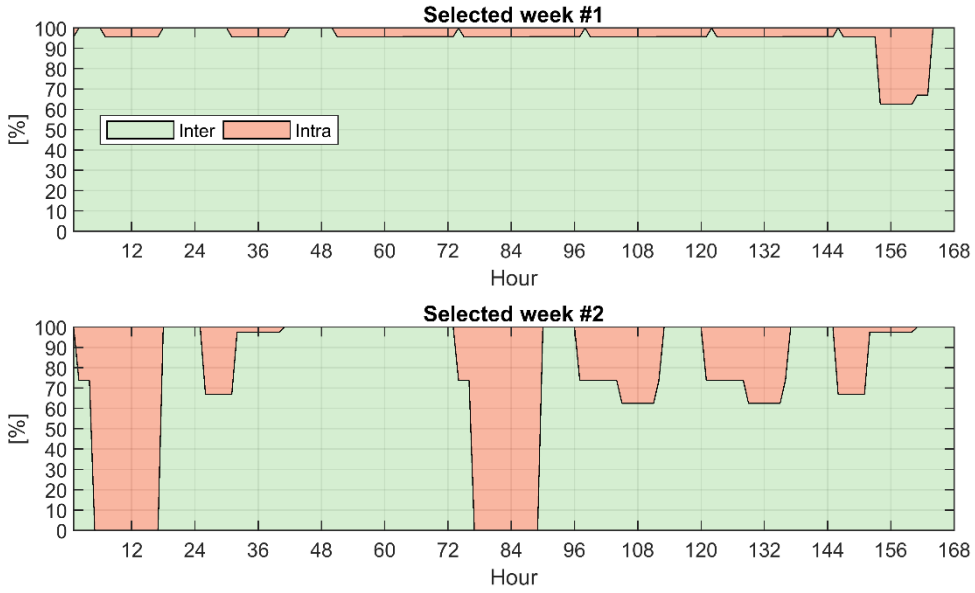

Fig. 8. Share of Inter/Intra Values in total Opportunity Cost of BESS

Another important aspect to discuss is that the coordination of short- and medium-term hydrothermal models has been traditionally performed by using two separate models and sharing information between them as in [34] and more recently in [35]. One medium-term model is run first using a reduced chronology, such as the LDC model described in Appendix B, in order to obtain the end volume or the water value from each reservoir. Under the assumption that a Stochastic Dual Dynamic Programming (SDDP) [36] approach has been used to solve the medium-term model, a piecewise-linear Future Cost Function (FCF) can be utilized to meet end-point conditions from the medium-term model in the short-term model as it was formerly proposed in [37] and more lately in [38]. This information is used as input data in a short-term model to find the daily levels and hourly opportunity costs. Finally, the LRP model is also compatible with decomposition techniques, such as Benders' decomposition or SDDP, in order to consider a large number of scenarios in the scenario tree. Therefore, it could be obtained the FCF internalizing the hourly dynamics of short-term storage, which is not possible with the current LDC model approach.

8. Conclusion

This paper introduces a novel formulation for stochastic hydrothermal models in which short-term opportunity costs are included in the medium- and long-optimization process. It has been validated the initial hypothesis, that short-term energy storage (e.g., BESS) decisions on energy production impact the opportunity cost (or water value) of seasonal storage. In the presented case study, in a comparison with a detailed hourly model used as benchmark, the classic LDC approach systematically underestimates the water value between 6% and 24% for seasonal hydro reservoirs, while the proposed LRP model error varies between 0% and 6.6%, sometimes underestimating and others overestimating. In addition, operational results (e.g., productions, number of cycles for short-term storage,

and storage levels) have a better estimation in the LRP model than in the LDC model. Another advantage of the proposed model is the possibility to obtain hourly detailed opportunity costs of ESS without solving an hourly hydrothermal dispatch model. Moreover, the proposed model formulation allows to differentiate between the short- and long-term opportunity costs. For instance, the results show that depending on the hour, the intra-period storage value (short-term opportunity cost) constitutes up to 100% of the total opportunity cost, demonstrating that inter-period opportunity cost may be also relevant for the long-term storage value. The derivation of an hourly opportunity cost of ESS that accounts for both short- and long-term dynamics represents a novel contribution, as it is not possible to obtain its value from a classic LDC model. In addition, the temporal reduction using the linked representative periods in the proposed LRP model makes it also suitable to solve real-size case studies. Furthermore, long-term opportunity costs due to hydro seasonality in power system internalize the hourly opportunity costs. In other words, the water value in seasonal storage includes the impact of short-term operational decisions.

This result is important to help market participants or planning authorities in their decision-making processes (bids or investment decisions in storage assets) by determining correct opportunity costs (i.e., short-term prices and long-term expected values) with the co-optimization approach in the LRP model and therefore avoiding sub-optimal solutions from iterative processes (e.g., fixing the hydro reservoirs levels obtained from a medium-term model in a short-term operational model).

Looking forward, the LRP model could be applied to analyze energy and operating reserve markets in hydrothermal power systems in a more natural way than using the LDC approach.

Appendix A. Hourly Unit Commitment Model

The following equations describe the hourly UC model used as the benchmark to test the proposed models, which is a simplified version of the model in ref. [39] including the hydrothermal constraints in ref. [40].

$$\min \sum_{\omega pt} p_p^{\omega} \cdot su_t \cdot SU_{pt}^{\omega} + \sum_{\omega pt} p_p^{\omega} \cdot sd_t \cdot SD_{pt}^{\omega} + \sum_{\omega pt} p_p^{\omega} \cdot f_t \cdot UC_{pt}^{\omega} + \sum_{\omega pt} p_p^{\omega} \cdot v_t \cdot P_{pt}^{\omega} + \sum_{\omega p} p_p^{\omega} \cdot v^{'} \cdot ENS_p^{\omega} + \sum_{\omega p} p_p^{\omega} \cdot v^{''} \cdot RNS_p^{\omega} \quad \text{(A.1)}$$

Subject to:

$$\sum_g O_{pg}^{\omega} + RNS_p^{\omega} \geq o_p \; \forall \omega p \quad \text{(A.2)}$$

$$\sum_g P_{pg}^{\omega} - \sum_s \frac{C_{ps}^{\omega}}{\eta_s} + ENS_p^{\omega} = d_p \; \forall \omega p \quad \text{(A.3)}$$

$$UC_{pt}^{\omega} - UC_{p-1t}^{\omega^{'}} = SU_{pt}^{\omega} - SD_{pt}^{\omega} \; \forall \omega pt \; \omega^{'} \epsilon \, a(\omega) \quad \text{(A.4)}$$

$$P_{pt}^{'\omega} + O_{pt}^{\omega} \leq (\overline{p}_t - \underline{p}_t) \cdot \left(UC_{pt}^{\omega} - SU_{pt}^{\omega}\right) \forall \omega pt \quad \text{(A.5)}$$

$$P_{pt}^{'\omega} + O_{pt}^{\omega} \leq (\overline{p}_t - \underline{p}_t) \cdot \left(UC_{pt}^{\omega} - SD_{p+1t}^{\omega}\right) \forall \omega pt \quad \text{(A.6)}$$

$$P_{pt}^{\omega} = \underline{p}_t \cdot UC_{pt}^{\omega} + P'^{\omega}_{pt} \quad \forall \omega p t \tag{A.7}$$

$$P_{ph}^{\omega} \leq \overline{p}_h \quad \forall \omega p h \tag{A.8}$$

$$R_{p-1r}^{intra,\omega'} - R_{pr}^{intra,\omega} + i_{pr}^{\omega} - S_{pr}^{\omega} + \underbrace{\sum_{r' \in RUR_{r',r}} S_{pr'}^{\omega}}_{\text{Water spillage from upstream reservoirs}} + \underbrace{\sum_{h \in HUR_{h,r}} P_{ph}^{\omega} / c_h}_{\text{Turbined water from upstream hydro plants}} - \underbrace{\sum_{h \in RUH_{r,h}} P_{ph}^{\omega} / c_h}_{\text{Turbined water from hydro plants in reservoir } r} + \underbrace{\sum_{h \in HPR_{h,r}} C_{ph}^{\omega} / c_h}_{\text{Pumped water from hydro plants to reservoir } r} - \underbrace{\sum_{h \in RPH_{r,h}} C_{ph}^{\omega} / c_h}_{\text{Pumped water to other reservoirs}} = 0 \quad \forall \omega p r \ \ \omega' \epsilon\, a(\omega) \tag{A.9}$$

$$SoC_{p-1b}^{intra,\omega'} - SoC_{pb}^{intra,\omega} - P_{pb}^{\omega} + C_{pb}^{\omega} = 0 \quad \forall \omega p b \quad \omega' \epsilon\, a(\omega) \tag{A.10}$$

$$R_{|P|r}^{intra,\omega} = r'_r \quad \forall \omega r \tag{A.11}$$

$$\underline{r}_r \leq R_{pr}^{intra,\omega} \leq \overline{r}_r \quad \forall \omega p r \tag{A.12}$$

$$\underline{soc}_b \leq SoC_{pb}^{intra,\omega} \leq \overline{soc}_b \quad \forall \omega p b \tag{A.13}$$

$$0 \leq P_{pg}^{\omega} \leq \overline{p}_g \quad \forall \omega p g \tag{A.14}$$

$$0 \leq C_{ps}^{\omega} \leq \overline{p}_s \quad \forall \omega p s \tag{A.15}$$

$$UC_{pt}^{\omega}, SU_{pt}^{\omega}, SU_{pt}^{\omega} \in \{0,1\} \quad \forall \omega p t \tag{A.16}$$

The objective function (A.1) minimizes the expected operational costs. Constraints (A.2) and (A.3) represent the operating reserve and the demand-balance equations respectively. Equation (A.4) is the logical relationship among the binary variables for UC. Constraints (A.5) to (A.7) ensure thermal unit production is within minimum and maximum capacity, while (A.8) ensures it for hydro units. Also, (A.9) defines the water balance for each reservoir considering the hydro topology. Constraint (A.10) defines the state of charge for each short-term ESS (e.g., batteries). Notice that constraints (A.9) and (A.10) are equivalent if, for example, a hydro reservoir has a pump unit which is not in a hydro basin and it has no hydro inflows. Constraint (A.11) establishes the final reservoir level at the last period of the time horizon. Equations (A.12) to (A.15) maintain bounds for the reservoir level, the state of charge, the power output, and the charged power per storage unit. Finally, (A.16) states that the commitment and connection variables are binary.

Appendix B. Load Duration Curve Model

This section shows the load levels formulation based on the modeling of hydrothermal dispatch problem in [40].

$$\min \ \sum_{\omega mwt} p_m^{\omega} \cdot su_t \cdot SU_{mwt}^{\omega} + \sum_{\omega mwt} p_m^{\omega} \cdot sd_t \cdot SD_{mwt}^{\omega} + \sum_{\omega mwlt} p_m^{\omega} \cdot wg_{mwl} \cdot f_t \cdot UC_{mwt}^{\omega} + \sum_{\omega mwlt} p_m^{\omega} \cdot wg_{mwl} \cdot v_t \cdot P_{mwlt}^{\omega} + \sum_{\omega mwl} p_m^{\omega} \cdot wg_{mwl} \cdot v' \cdot ENS_{mwl}^{\omega} + \sum_{\omega mwl} p_m^{\omega} \cdot wg_{mwl} \cdot v'' \cdot RNS_{mwl}^{\omega} \tag{B.1}$$

Subject to:

$$\sum_g O_{mwlg}^{\omega} + RNS_{mwl}^{\omega} \geq o_{mwl} \quad \forall \omega m w l \tag{B.2}$$

$$\sum_g P^{\omega}_{mwlg} - \sum_s \frac{C^{\omega}_{mwls}}{\eta_s} + ENS^{\omega}_{mwl} = d_{mwl} \quad \forall \omega mwl \tag{B.3}$$

$$P^{\omega}_{mwl+1g} \leq P^{\omega}_{mwlg} \quad \forall \omega mwlg \tag{B.4}$$

$$UC^{\omega}_{mwt} - UC^{\omega'}_{m-1w+1t} = SU^{\omega}_{mwt} - SD^{\omega}_{mwt} \quad \forall \omega mwt \quad \omega' \epsilon\, a(\omega) \tag{B.5}$$

$$UC^{\omega}_{mw+1t} - UC^{\omega}_{mwt} = SU^{\omega}_{mw+1t} - SD^{\omega}_{mw+1t} \quad \forall \omega mt\ \forall w > 1 \tag{B.6}$$

$$P^{\omega}_{mwlt} + O^{\omega}_{mwlt} \leq \overline{p}_t UC^{\omega}_{mwt} \quad \forall \omega mwt \tag{B.7}$$

$$P^{\omega}_{mwlt} \geq \underline{p}_t UC^{\omega}_{mwt} \quad \forall \omega mwt \tag{B.8}$$

$$P^{\omega}_{mwlh} \leq \overline{p}_h \quad \forall \omega mwh \tag{B.9}$$

$$R^{inter,\omega'}_{m-1r} - R^{inter,\omega}_{mr} + i^{\omega}_{mr} - S^{\omega}_{mr} + \underbrace{\sum_{r' \in RUR_{r',r}} S^{\omega'}_{mr'}}_{\text{Water spillage from upstream reservoirs}} + \underbrace{\sum_{wl}\sum_{h \in HUR_{h,r}} {wg_{mwl} \cdot P^{\omega}_{mwlh}}/{c_h}}_{\text{Turbined water from upstream hydro plants}} \tag{B.10}$$

$$- \underbrace{\sum_{wl}\sum_{h \in RUH_{r,h}} {wg_{mwl} \cdot P^{\omega}_{mwlh}}/{c_h}}_{\text{Turbined water from hydro plants in reservoir } r} + \underbrace{\sum_{wl}\sum_{h \in HPR_{h,r}} {wg_{mwl} \cdot C^{\omega}_{mwlh}}/{c_h}}_{\text{Pumped water from hydro plants to reservoir } r} -$$

$$\underbrace{\sum_{wl}\sum_{h \in RPH_{r,h}} {wg_{mwl} \cdot C^{\omega}_{mwlh}}/{c_h}}_{\text{Pumped water to other reservoirs}} = 0 \quad \forall \omega mr \quad \omega' \epsilon\, a(\omega)$$

$$SoC^{inter,\omega'}_{m-1b} - SoC^{inter,\omega}_{mb} - \sum_{wl} wg_{mwl} \cdot P^{\omega}_{mwlb} + \sum_{wl} wg_{mwl} \cdot C^{\omega}_{mwlb} = 0 \quad \forall \omega mb \quad \omega' \epsilon\, a(\omega) \tag{B.11}$$

$$R^{inter,\omega}_{|M|r} = r'_r \quad \forall \omega r \tag{B12}$$

$$\underline{r}_r \leq R^{inter,\omega}_{mr} \leq \overline{r}_r \quad \forall \omega mr \tag{B.13}$$

$$\underline{soc}_b \leq SoC^{inter,\omega}_{mb} \leq \overline{soc}_b \quad \forall \omega mb \tag{B.14}$$

$$0 \leq P^{\omega}_{mwlg} \leq \overline{p}_g \quad \forall \omega mwg \tag{B.15}$$

$$0 \leq C^{\omega}_{mwls} \leq \overline{p}_s \quad \forall \omega mws \tag{B.16}$$

$$UC^{\omega}_{mwt}, SU^{\omega}_{mwt}, SU^{\omega}_{mwt} \in \{0,1\} \quad \forall \omega mwt \tag{B.17}$$

The objective function (B.1) minimizes the expected operational costs such as (A.1) in the HM model. Constraints (B.2) to (B.17) have the same purpose as in the HM model. However, they are stated in term of the LDC time division, i.e., m,w,l.

Moreover, the following considerations are particular for the LDC model: Equation (B.4) limits the production in consecutive load levels. Equations (B.5) and (B.6) represent the commitment constraints in the LDC model. This model considers startup and shutdown decisions within aggregation of load levels w. For instance, if the aggregations of load levels are weekdays and weekend, then equations (B.5) and (B.6) define the commitment, startup, and shutdown decisions between weekdays and the following weekend and vice versa.

Equation (B.10) defines the water balance for each reservoir considering the hydro topology while (B.11) defines the state of charge for each short-term storage (e.g., batteries).

Appendix C. Linked Representative Periods Model

This section describes the LRP model, which is a stochastic extension of the previous formulation developed in [20]. This model is a novel contribution to hydrothermal dispatch because it enables consideration of both short-term storage (e.g., batteries) and seasonal storage simultaneously.

$$\min \sum_{\omega m} p_m^{\omega} \sum_{rp,k,t} wg_{rp} \cdot su_t \cdot SU_{rp,k,t}^{\omega} + \sum_{\omega m} p_m^{\omega} \sum_{t,\,(rp,k) \in \{CI_{p,rp,k} \cap MP_{m,p}\}} wg_{rp} \cdot sd_t \cdot SD_{rp,k,t}^{\omega} + \sum_{\omega m} p_m^{\omega} \sum_{t,\,(rp,k) \in \{CI_{p,rp,k} \cap MP_{m,p}\}} wg_{rp} \cdot f_t \cdot UC_{rp,k,t}^{\omega} + \sum_{\omega m} p_m^{\omega} \sum_{t,\,(rp,k) \in \{CI_{p,rp,k} \cap MP_{m,p}\}} wg_{rp} \cdot v_t \cdot P_{rp,k,t}^{\omega} + \sum_{\omega m} p_m^{\omega} \sum_{(rp,k) \in \{CI_{p,rp,k} \cap MP_{m,p}\}} wg_{rp} \cdot v^{'} \cdot ENS_{rp,k}^{\omega} + \sum_{\omega m} p_m^{\omega} \sum_{(rp,k) \in \{CI_{p,rp,k} \cap MP_{m,p}\}} wg_{rp} \cdot v^{''} \cdot RNS_{rp,k}^{\omega} \quad \text{(C.1)}$$

Subject to:

$$\sum_g O_{rp,k,g}^{\omega} + RNS_{rp,k}^{\omega} \geq o_{rp,k} \quad \forall \omega, rp, k \quad \text{(C.2)}$$

$$\sum_g P_{rp,k,g}^{\omega} - \sum_s \frac{C_{rp,k,s}^{\omega}}{\eta_s} + ENS_{rp,k}^{\omega} = d_{rp,k} \quad \forall \omega, rp, k \quad \text{(C.3)}$$

$$UC_{rp,k,t}^{\omega} - UC_{rp,k-1,t}^{\omega} = SU_{rp,k,t}^{\omega} - SD_{rp,k,t}^{\omega} \quad \forall \omega, rp, t \; \forall k > 1 \quad \text{(C.4)}$$

$$UC_{rp,k,t}^{\omega} - \sum_{rp^{'} \in TM_{rp^{'},rp}} UC_{rp^{'},K,t}^{\omega^{'}} = SU_{rp,k,t}^{\omega} - SD_{rp,k,t}^{\omega} \quad \forall \omega, rp, t \quad \forall k = 1 \quad \omega^{'} \epsilon \, a(\omega) \quad \text{(C.5)}$$

$$P_{rp,k,t}^{'\omega} + O_{rp,k,t}^{\omega} \leq (\overline{p}_t - \underline{p}_t) \cdot \left(UC_{rp,k,t}^{\omega} - SU_{rp,k,t}^{\omega}\right) \quad \forall \omega, rp, k, t \quad \text{(C.6)}$$

$$P_{rp,k,t}^{'\omega} + O_{rp,k,t}^{\omega} \leq (\overline{p}_t - \underline{p}_t) \cdot \left(UC_{rp,k,t}^{\omega} - SD_{rp,k+1,t}^{\omega}\right) \quad \forall \omega, rp, k, t \quad \text{(C.7)}$$

$$P_{rp,k,t}^{\omega} = \underline{p}_t UC_{rp,k,t}^{\omega} + P_{rp,k,t}^{'\omega} \quad \forall \omega, rp, k, t \quad \text{(C.8)}$$

$$P_{rp,k,h}^{\omega} \leq \overline{p}_h \quad \forall \omega, rp, k, h \quad \text{(C.9)}$$

$$R_{rp,k-1,r}^{intra,\omega^{'}} - R_{rp,k,r}^{intra,\omega} + i_{rp,k,r}^{\omega} - S_{rp,k,r}^{\omega} + \underbrace{\sum_{r^{'} \in RUR_{r^{'},r}} S_{rp,k,r^{'}}^{\omega}}_{Water\ spillage\ from\ upstream\ reservoirs} + \underbrace{\sum_{h \in HUR_{h,r}} P_{rp,k,h}^{\omega} / c_h}_{Turbined\ water\ from\ upstream\ hydro\ plants} - \underbrace{\sum_{h \in RUH_{r,h}} P_{rp,k,h}^{\omega} / c_h}_{Turbined\ water\ from\ hydro\ plants\ in\ reservoir\ r} + \underbrace{\sum_{h \in HPR_{h,r}} C_{rp,k,h}^{\omega} / c_h}_{Pumped\ water\ from\ hydro\ plants\ to\ reservoir\ r} - \underbrace{\sum_{h \in RPH_{r,h}} C_{rp,k,h}^{\omega} / c_h}_{Pumped\ water\ to\ other\ reservoirs} = 0 \quad \forall \omega, rp, k, r \quad \omega^{'} \epsilon \, a(\omega) \quad \text{(C.10)}$$

$$R_{m-1,r}^{inter,\omega^{'}} - R_{mr}^{inter,\omega} + \sum_{(rp,k) \in \{CI_{p,rp,k} \cap MP_{m,p}\}} \left[R_{rp,k,r}^{intra,\omega} - R_{rp,k-1,r}^{intra,\omega^{'}}\right] = 0 \quad \forall \omega m r \quad \omega^{'} \epsilon \, a(\omega) \quad \text{(C.11)}$$

$$SoC_{rp,k-1,b}^{intra,\omega^{'}} - SoC_{rp,k,b}^{intra,\omega} - P_{rp,k,b}^{\omega} + C_{rp,k,b}^{\omega} = 0 \quad \forall \omega, rp, k, b \quad \omega^{'} \epsilon \, a(\omega) \quad \text{(C.12)}$$

$$SoC_{m-1,b}^{inter,\omega^{'}} - SoC_{mb}^{inter,\omega} + \sum_{(rp,k) \in \{CI_{p,rp,k} \cap MP_{m,p}\}} \left[SoC_{rp,k,r}^{intra,\omega} - SoC_{rp,k-1,r}^{intra,\omega^{'}}\right] = 0 \quad \forall \omega m b \quad \omega^{'} \epsilon \, a(\omega) \quad \text{(C.13)}$$

$$R_{|M|r}^{inter,\omega} = r_r^{'} \quad \forall \omega r \quad \text{(C.14)}$$

$$\underline{r}_r \leq R_{mr}^{inter,\omega} \leq \overline{r}_r \quad \forall \omega m r \quad \text{(C.15)}$$

$$\underline{r}_r \leq R_{rp,k,r}^{intra,\omega} \leq \overline{r}_r \quad \forall \omega, rp, k, r \quad \text{(C.16)}$$

$$\underline{soc}_b \leq SoC_{mb}^{inter,\omega} \leq \overline{soc}_b \quad \forall \omega m b \quad \text{(C.17)}$$

$$\underline{soc}_b \leq SoC_{rp,k,b}^{intra,\omega} \leq \overline{soc}_b \quad \forall \omega, rp, k, b \quad \text{(C.18)}$$

$$0 \leq P_{rp,k,g}^{\omega} \leq \overline{p}_g \quad \forall \omega, rp, k, g \quad \text{(C.19)}$$

$$0 \leq C_{rp,k,s}^{\omega} \leq \overline{p}_s \quad \forall \omega, rp, k, s \quad \text{(C.20)}$$

$UC^{\omega}_{rp,k,t}, SU^{\omega}_{rp,k,t}, SU^{\omega}_{rp,k,t} \in \{0,1\} \quad \forall \omega,rp,k,t$ (C.21)

The objective function (C.1) also minimizes the expected operational costs such as (A.1) in the HM model. The operational costs associated with each RP are multiplied by the number of periods in the time horizon that are represented by it, i.e., multiplied by the weight of each RP. In addition, the intersection of both sets $\{CI_{p,rp,k} \cap MP_{m,p}\}$ guarantees that it is considering only the RPs belonging to the corresponding month. Constraints (C.2) to (C.21) have the same purpose as their equivalent ones in the HM model. However, they are stated in term of the RPs time division, i.e., rp,k.

Moreover, the following considerations are specific to the LRP model: Equations (C.4) and (C.5) are the commitment constraints in the LRP model. Equation (C.4) is for all the hours inside the RP except for the first hour. For the first hour, (C.5) creates continuity between the RPs and prevents unnecessary startups by using a transition matrix, i.e., $TM_{rp',rp}$, to require that for any pair of RPs that transition from one to the other, the thermal unit status in the last hour of the first, i.e., rp', is considered in the first hour of the second, i.e., rp.

Equations (C.10) to (c.13) represent the balance equations for both types of storage, i.e., hydro reservoirs and batteries. These equations create the continuity in storage across the entire time horizon that allows for the modeling of short-term and long-term storage simultaneously.

References

[1] Huber M, Dimkova D, Hamacher T. Integration of wind and solar power in Europe: Assessment of flexibility requirements. Energy 2014;69:236–46. doi:10.1016/j.energy.2014.02.109.

[2] Ma J, Silva V, Belhomme R, Kirschen DS, Ochoa LF. Evaluating and Planning Flexibility in Sustainable Power Systems. IEEE Transactions on Sustainable Energy 2013;4:200–9. doi:10.1109/TSTE.2012.2212471.

[3] Strbac G, Aunedi M, Konstantelos I, Moreira R, Teng F, Moreno R, et al. Opportunities for Energy Storage: Assessing Whole-System Economic Benefits of Energy Storage in Future Electricity Systems. IEEE Power and Energy Magazine 2017;15:32–41. doi:10.1109/MPE.2017.2708858.

[4] Pérez-Díaz JI, Jiménez J. Contribution of a pumped-storage hydropower plant to reduce the scheduling costs of an isolated power system with high wind power penetration. Energy 2016;109:92–104. doi:10.1016/j.energy.2016.04.014.

[5] Wogrin S, Gayme DF. Optimizing Storage Siting, Sizing, and Technology Portfolios in Transmission-Constrained Networks. IEEE Transactions on Power Systems 2015;30:3304–13. doi:10.1109/TPWRS.2014.2379931.

[6] Poncelet K, Höschle H, Delarue E, Virag A, D'haeseleer W. Selecting Representative Days for Capturing the Implications of Integrating Intermittent Renewables in Generation Expansion Planning Problems. IEEE Transactions on Power Systems 2017;32:1936–48. doi:10.1109/TPWRS.2016.2596803.

[7] Moreno R, Ferreira R, Barroso L, Rudnick H, Pereira E. Facilitating the Integration of Renewables in Latin America: The Role of Hydropower Generation and Other Energy Storage Technologies. IEEE Power and Energy Magazine 2017;15:68–80. doi:10.1109/MPE.2017.2708862.

[8] Sherkat VR, Campo R, Moslehi K, Lo EO. Stochastic Long-Term Hydrothermal Optimization for a Multireservoir System. IEEE Transactions on Power Apparatus and Systems 1985;PAS-104:2040–50. doi:10.1109/TPAS.1985.318779.

[9] Zhang H, Zhou J, Fang N, Zhang R, Zhang Y. Daily hydrothermal scheduling with economic emission using simulated annealing technique based multi-objective cultural differential evolution approach. Energy 2013;50:24–37. doi:10.1016/j.energy.2012.12.001.

[10] Matos VL de, Finardi EC. A computational study of a stochastic optimization model for long term hydrothermal scheduling. International Journal of Electrical Power & Energy Systems 2012;43:1443–52. doi:10.1016/j.ijepes.2012.06.021.

[11] de Queiroz AR. Stochastic hydro-thermal scheduling optimization: An overview. Renewable and Sustainable Energy Reviews 2016;62:382–95. doi:10.1016/j.rser.2016.04.065.
[12] Maceira MEP, Duarte V, Penna D, Moraes L, Melo A. Ten years of application of stochastic dual dynamic programming in official and agent studies in brazil-description of the newave program. 16th PSCC, Glasgow, Scotland 2008:14–18.
[13] Cerisola S, Latorre JM, Ramos A. Stochastic dual dynamic programming applied to nonconvex hydrothermal models. European Journal of Operational Research 2012;218:687–97. doi:10.1016/j.ejor.2011.11.040.
[14] Wogrin S, Duenas P, Delgadillo A, Reneses J. A New Approach to Model Load Levels in Electric Power Systems With High Renewable Penetration. IEEE Transactions on Power Systems 2014;29:2210–8. doi:10.1109/TPWRS.2014.2300697.
[15] Zheng JH, Chen JJ, Wu QH, Jing ZX. Reliability constrained unit commitment with combined hydro and thermal generation embedded using self-learning group search optimizer. Energy 2015;81:245–54. doi:10.1016/j.energy.2014.12.036.
[16] Nahmmacher P, Schmid E, Hirth L, Knopf B. Carpe diem: A novel approach to select representative days for long-term power system modeling. Energy 2016;112:430–42. doi:10.1016/j.energy.2016.06.081.
[17] Koltsaklis NE, Georgiadis MC. A multi-period, multi-regional generation expansion planning model incorporating unit commitment constraints. Applied Energy 2015;158:310–31. doi:10.1016/j.apenergy.2015.08.054.
[18] Kotzur L, Markewitz P, Robinius M, Stolten D. Time series aggregation for energy system design: Modeling seasonal storage. Applied Energy 2018;213:123–35. doi:10.1016/j.apenergy.2018.01.023.
[19] Pineda S, Morales JM. Chronological time-period clustering for optimal capacity expansion planning with storage. IEEE Transactions on Power Systems 2018:1–1. doi:10.1109/TPWRS.2018.2842093.
[20] Tejada-Arango DA, Domeshek M, Wogrin S, Centeno E. Enhanced Representative Days and System States Modeling for Energy Storage Investment Analysis. IEEE Transactions on Power Systems 2018;33:6534–44. doi:10.1109/TPWRS.2018.2819578.
[21] Fazlollahi S, Bungener SL, Mandel P, Becker G, Maréchal F. Multi-objectives, multi-period optimization of district energy systems: I. Selection of typical operating periods. Computers & Chemical Engineering 2014;65:54–66. doi:10.1016/j.compchemeng.2014.03.005.
[22] Reichenberg L, Siddiqui AS, Wogrin S. Policy implications of downscaling the time dimension in power system planning models to represent variability in renewable output. Energy 2018;159:870–7. doi:10.1016/j.energy.2018.06.160.
[23] Sisternes FJD, Webster MD, Sisternes OJD, Webster MD. Optimal Selection of Sample Weeks for Approximating the Net Load in Generation Planning Problems 2013.
[24] Latorre JM, Cerisola S, Ramos A. Clustering algorithms for scenario tree generation: Application to natural hydro inflows. European Journal of Operational Research 2007;181:1339–53. doi:10.1016/j.ejor.2005.11.045.
[25] Oliveira WL de, Sagastizábal C, Penna DDJ, Maceira MEP, Damázio JM. Optimal scenario tree reduction for stochastic streamflows in power generation planning problems. Optimization Methods and Software 2010;25:917–36. doi:10.1080/10556780903420135.
[26] Shapiro A. Analysis of stochastic dual dynamic programming method. European Journal of Operational Research 2011;209:63–72. doi:10.1016/j.ejor.2010.08.007.
[27] Reneses J, Barquín J, García-González J, Centeno E. Water value in electricity markets. International Transactions on Electrical Energy Systems 2016;26:655–70. doi:10.1002/etep.2106.
[28] Razavi S-E, Esmaeel Nezhad A, Mavalizadeh H, Raeisi F, Ahmadi A. Robust hydrothermal unit commitment: A mixed-integer linear framework. Energy 2018;165:593–602. doi:10.1016/j.energy.2018.09.199.
[29] ENTSO-E. Ten Year Network Development Plan 2016 2016. http://tyndp.entsoe.eu/ (accessed August 3, 2017).
[30] Staffell I, Pfenninger S. Using bias-corrected reanalysis to simulate current and future wind power output. Energy 2016;114:1224–39. doi:10.1016/j.energy.2016.08.068.
[31] Pfenninger S, Staffell I. Long-term patterns of European PV output using 30 years of validated hourly reanalysis and satellite data. Energy 2016;114:1251–65. doi:10.1016/j.energy.2016.08.060.
[32] PSR – Energy Consulting and Analytics. SDDP – Stochastic hydrothermal dispatch with network restrictions. Software | PSR – Energy Consulting and Analytics 2018. https://www.psr-inc.com/softwares-en/ (accessed May 9, 2018).
[33] Tejada-Arango DA, Wogrin S, Centeno E. Representation of Storage Operations in Network-Constrained Optimization Models for Medium- and Long-Term Operation. IEEE Transactions on Power Systems 2018;33:386–96. doi:10.1109/TPWRS.2017.2691359.
[34] Pereira MVF, Pinto LMVG. A Decomposition Approach to the Economic Dispatch of Hydrothermal Systems. IEEE Transactions on Power Apparatus and Systems 1982;PAS-101:3851–60. doi:10.1109/TPAS.1982.317035.
[35] Bregadioli GF, Baptista EC, Nepomuceno L, Balbo AR, Soler EM. Medium-term coordination in a network-constrained multi-period auction model for day-ahead markets of hydrothermal systems. International Journal of Electrical Power & Energy Systems 2016;82:474–83. doi:10.1016/j.ijepes.2016.03.032.

[36] Maceiral M, Penna D, Diniz A, Pinto R, Melo A, Vasconcellos C, et al. Twenty Years of Application of Stochastic Dual Dynamic Programming in Official and Agent Studies in Brazil-Main Features and Improvements on the NEWAVE Model. 2018 Power Systems Computation Conference (PSCC), IEEE; 2018, p. 1–7.
[37] Gorenstin BG, Campodonico NM, Costa JP da, Pereira MVF. Stochastic optimization of a hydro-thermal system including network constraints. IEEE Transactions on Power Systems 1992;7:791–7. doi:10.1109/59.141787.
[38] Alvarez M, Rönnberg SK, Bermúdez J, Zhong J, Bollen MHJ. Reservoir-type hydropower equivalent model based on a future cost piecewise approximation. Electric Power Systems Research 2018;155:184–95. doi:10.1016/j.epsr.2017.09.028.
[39] Morales-Espana G, Latorre JM, Ramos A. Tight and Compact MILP Formulation for the Thermal Unit Commitment Problem. IEEE Transactions on Power Systems 2013;28:4897–908. doi:10.1109/TPWRS.2013.2251373.
[40] Andrés Ramos Galán, Antonio Alonso Ayuso, Gloria Pérez Sainz de Rozas. Optimización bajo incertidumbre. Universidad Pontificia Comillas; 2008.

Conflict of Interest and Authorship Conformation Form

Please check the following as appropriate:

X All authors have participated in (a) conception and design, or analysis and interpretation of the data; (b) drafting the article or revising it critically for important intellectual content; and (c) approval of the final version.

X This manuscript has not been submitted to, nor is under review at, another journal or other publishing venue.

X The authors have no affiliation with any organization with a direct or indirect financial interest in the subject matter discussed in the manuscript

o The following authors have affiliations with organizations with direct or indirect financial interest in the subject matter discussed in the manuscript:

Author's name	Affiliation

Highlights

- Representation of short-term operational decisions in hydrothermal dispatch models.
- Integration of short-term storage (e.g., batteries) drives this representation.
- This paper compares two models: classic Load Duration Curve vs Linked-Representative Periods.
- The Linked-Representative Periods model can determine hourly opportunity costs for short-term energy storage.
- These types of results cannot be obtained in the classic Load Duration Curve model.